

# Application of Rapid Prototyping Technique and Intraoperative Navigation System for the Repair and Reconstruction of Orbital Wall Fractures

Jong Hyun Cha<sup>1</sup>,  
Yong Hae Lee<sup>1</sup>,  
Wan Chul Ruy<sup>1</sup>,  
Young Roe<sup>2</sup>,  
Myung Ho Moon<sup>3</sup>,  
Sung Gyun Jung<sup>4</sup>

<sup>1</sup>Department of Plastic and Reconstructive Surgery, Konyang University College of Medicine, Daejeon;

<sup>2</sup>Department of Plastic and Reconstructive Surgery, Inha University School of Medicine, Incheon;

<sup>3</sup>Biomedical Engineering, Konyang University College of Medicine, Daejeon;

<sup>4</sup>Department of Plastic and Reconstructive Surgery, National Medical Center, Seoul, Korea

No potential conflict of interest relevant to this article was reported.

**Background:** Restoring the orbital cavity in large blow out fractures is a challenge for surgeons due to the anatomical complexity. This study evaluated the clinical outcomes and orbital volume after orbital wall fracture repair using a rapid prototyping (RP) technique and intraoperative navigation system.

**Methods:** This prospective study was conducted on the medical records and radiology records of 12 patients who had undergone a unilateral blow out fracture reconstruction using a RP technique and an intraoperative navigation system from November 2014 to March 2015. The surgical results were assessed by an ophthalmic examination and a comparison of the preoperative and postoperative orbital volume ratio (OVR) values.

**Results:** All patients had a successful treatment outcome without complications. Volumetric analysis revealed a significant decrease in the mean OVR from 1.0952±0.0662 (ranging from 0.9917 to 1.2509) preoperatively to 0.9942±0.0427 (ranging from 0.9394 to 1.0680) postoperatively.

**Conclusion:** The application of a RP technique for the repair of orbital wall fractures is a useful tool that may help improve the clinical outcomes by understanding the individual anatomy, determining the operability, and restoring the orbital cavity volume through optimal implant positioning along with an intraoperative navigation system.

**Keywords:** Pinting / Three-dimensional / Computer simulation / Orbital fractures

## INTRODUCTION

Orbital fractures account for approximately 40% of craniofacial traumas. A large portion of orbital cavity fractures often occurs in the orbital inferior wall, in the infraorbital groove and canal, and in the medial orbital wall [1-4]. These bony fractures can alter cavity dimensions and shift the position of intraorbital contents, resulting in diplopia, enophthalmos, and visual acuity disturbances [4]. Res-

toration of the orbit to its preinjury anatomy is important for preventing complications, and studies have described a range of methods, such as transconjunctival, subciliary, and coronal approaches, as well as a diversity of graft and reconstructive materials, including bones, cartilage, titanium, and resorbable mesh. Nevertheless, postoperative complications are not infrequent and include diplopia, infraorbital nerve dysfunction, enophthalmos, and malposition of the reconstruction materials due to the structural complexity of the orbit, the restricted field of view, injuries to the neighboring tissues, any other causes as well [5]. Having a good understanding of the disrupted orbital anatomy and injury severity may positively affect the surgical procedure and help improve the potential outcome.

Rapid prototyping (RP), which uses digital signals to produce three-dimensional objects, was developed in the 1980s. This tech-

**Correspondence:** Sung Gyun Jung

Department of Plastic and Reconstructive Surgery, National Medical Center, 245 Eulji-ro, Jung-gu, Seoul 04564, Korea  
E-mail: sunggyun\_jung@hotmail.com

\*This article was presented at the 5th Research and Reconstructive Forum, in Pyeongchang, Korea

Received July 6, 2016 / Revised September 9, 2016 / Accepted September 10, 2016

nology has a wide spectrum of applications across many fields, such as science, industry, fashion, food, and medicine [6-8]. In the craniofacial field, reconstructive techniques using RP is highly applicable because of the structural complexity of craniofacial bones, particularly that of the orbital cavity [4,9,10]. An intraoperative navigation system can use the radiologic data as a map of the intraoperative condition, to help position the reconstruction materials accurately, decrease the rate of complications, and bring about a positive outcome [6,11].

The aim of this prospective study was to present a method of reconstructing unilateral orbital wall fractures using RP technique with intraoperative navigation system and assess its utility.

## METHODS

A prospective study was conducted for patients who had undergone unilateral blowout fracture reconstruction using the RP technique and intraoperative navigation system at a single academic institution between November, 2014 and March, 2015. The operator was one senior author, and the operative indications included (1) restriction of extraocular muscles, (2) radiologic evidence of an excessive fracture ( $2\text{ cm}^2$ ), (3) enophthalmos ( $>2\text{ mm}$ ), and (4) increased volume of the orbital cavity by more than 5%. A total of 12 patients underwent unilateral blowout fracture reconstruction using a RP technique and an intraoperative navigation system. Each patient received a cranial computed tomography (CT) scan and underwent preoperative evaluation by an ophthalmologist for diplopia, oculomotor movement dysfunction, enophthalmos, and other functional issues related to vision. Enophthalmos was defined as  $\geq 2\text{ mm}$  difference on Hertel Exophthalmometer. Primary diplopia was defined as severe and other types of diplopia were defined as mild [12]. Postoperatively, each patient received a CT scan. The injured orbit was compared with the contralateral, uninjured orbit for orbital tissues and orbital volume restored (Fig. 1). At one week, a postoperative ophthalmologic evaluation conducted for complications such as postoperative enophthalmos, diplopia, and oculomotor dysfunction.

## 3D printing technique

Using a preoperative CT scan, DICOM files of 0.5 mm in thickness were imported to a three-dimensional image processing software (Mimics 17.0, Materialise, Leuven, Belgium), and virtual 3D modeling was performed. Only the facial bones were presented in a threshold suitable for hard tissues and the patient's anatomical condition, and the size and location of the defects were determined by virtual 3D modeling to perform virtual 3D surgical planning (Fig. 2). To allow optimal coverage of the orbital cavity defects, virtual modeling of the injured orbital cavity and an image of the uninjured one were overlapped through mirroring, which provided a three-dimensional mark of an interface not overlapped due to defects, using a computer aided design (CAD) program (3-matic Research 9.0 Materialise, Belgium), and a guide implant was designed for optimal coverage of the defect site. The



**Fig. 1.** Preoperative and postoperative computed tomography (CT) scan images. The unilateral orbital wall fracture was reconstructed using a rapid prototyping technique and an intraoperative navigation system. (A) Preoperative and (B) postoperative CT scan image of inferomedial orbital wall fracture.

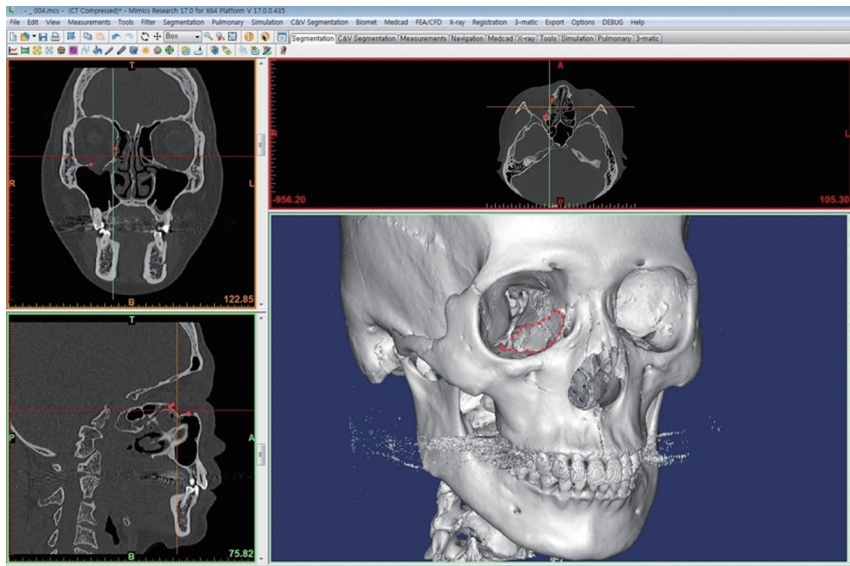


**Fig. 2.** Virtual 3D modeling of the orbital wall fracture. Virtual 3D modeling of the unilateral orbital wall fracture using 3D image processing software (Mimics 17.0, Materialise, Leuven, Belgium). The 3D mark to an interface was not overlapped due to defects compared to the image of the uninjured one through mirroring (red dot).

virtual 3D orbital model and the guide implant were transformed to a stereolithography file for 3D printing, and the orbital model was printed using fused deposition modeling (FDM, Fortus 360mc, Stratasys, Minnesota, USA) and the implant using Polyjet (Objet 500 connex2, Stratasys) (Fig. 3A).

### Orbital volume

Virtual 3D modeling was performed to assess the postoperative results, and three-dimensional measuring was used to determine the defect size as well as the orbital volume of both the injured and uninjured sites. When an orbital interface was not identified due to orbital wall defects at the fracture site, the orbital volume was measured on the interface of soft tissues. The postoperative orbital volume was measured based on the orbital and implant borders, and the volumetric ratio of the uninjured orbital cavity to the injured orbital cavity was used to reduce the gap in the volume among patients as well as the errors by the uninjured orbital volume (Fig. 4) [13].

Orbital volume ratio (OVR)=Injured orbital cavity volume/  
Uninjured orbital cavity volume.

### Surgical approach

Preoperatively, a 3D printed orbital RP model was used for surgical planning and was then sterilized for use in the operative field. Under general anesthesia, the fracture site was approached via an extended combined transconjunctival inferior fornix approach as well as through a retrocaruncular approach. With adequate visualization, the orbital periosteum was incised sharply and retracted. The region below the periosteum was explored carefully to view the blowout fractures with ease. After full exposure, the herniated orbital contents were released carefully into the surrounding spaces, including the maxillary sinus of the nasal cavity. The orbital wall was reconstructed with previously contoured hydroxyapatite mesh (Osteotrans Mx, Takiron, Kokyo, Japan). First, the hydroxyapatite mesh was fabricated with similar to normal orbital curvature by using the orbital RP model as template. Then, we trimmed the implant down using the implant RP model as a guide. The appropriateness of an implant to cover defects fully in an orbital cavity RP model was confirmed, and the landmark for positioning was identified. For optimal implant positioning, a surgical navigation system (StealthStation S7, Medtronic, Dublin, Ireland) was used to confirm the optimal coverage of the defect site by the customized implant.

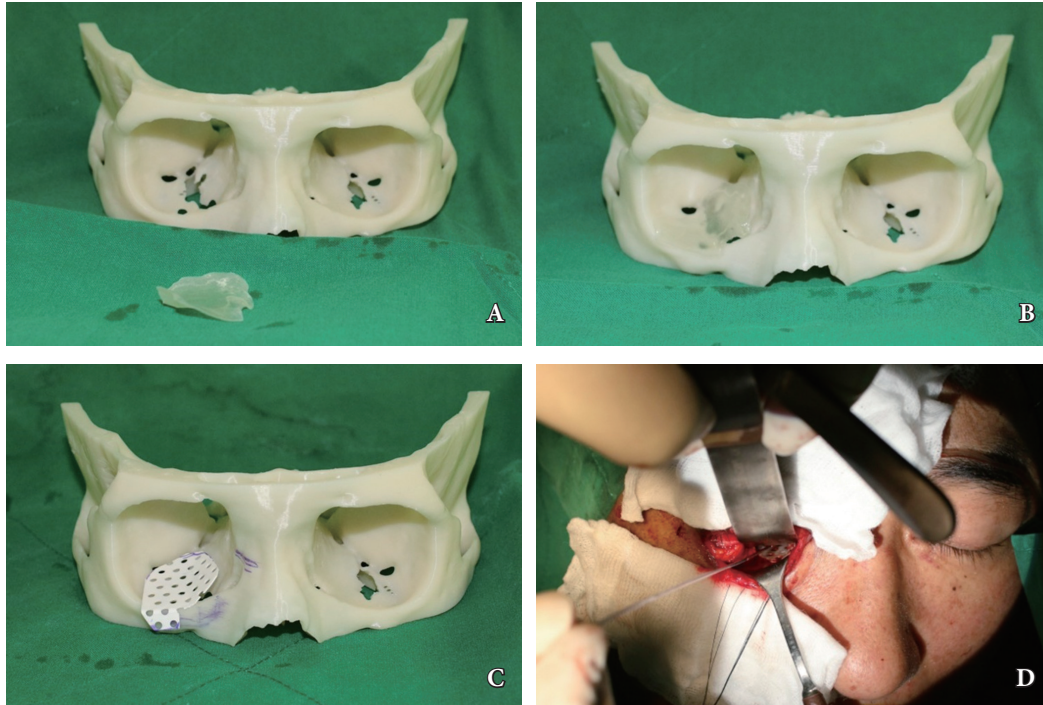


**Fig. 3.** Application of rapid prototyping (RP) model in operation field. (A) Orbital RP model with Guide Implant RP model, (B) Guide Implant RP model fit to the defect area of the inferomedial side on Orbital RP model, (C) Application of trimmed hydroxyapatite implant (Osteotrans Mx, Takiron, Tokyo, Japan) to the orbital RP model as a template, (D) application of the implant in operation field with Intraoperative Navigation System (StealthStation S7, Medtronic, Dublin, Ireland).

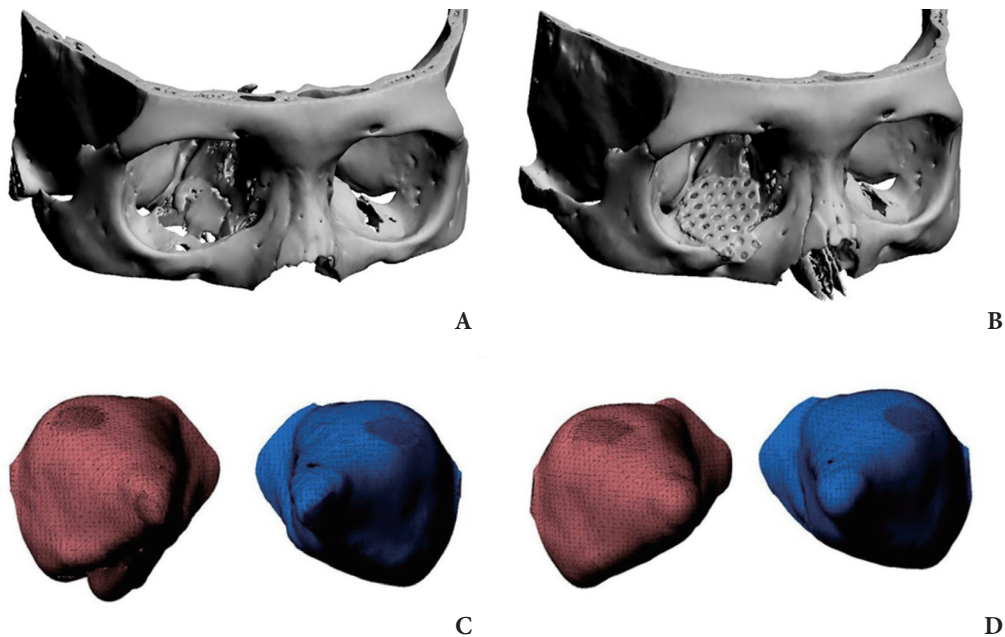


**Fig. 4.** Preoperative and postoperative 3D modeling and orbital volume. (A) Preoperative 3D modeling; right inferomedial blowout fracture, (B) Postoperative 3D modeling with the applied implant, (C) Preoperative 3D modeling of the orbital volume, (D) postoperative 3D modeling of the orbital volume; reduced orbital volume on the inferomedial area.



Intraoperative navigation was carried out by means of a navigation pointer via electromagnetic tracking system. The patient's position was identified with a digital reference frame that was registered using electromagnetic detector. Various points on the virtual image at the workstation and the patient were matched and compared with anatomic landmarks (Fig. 3). One or two absorbable hydroxyapatite screws (Osteotrans Mx, Takiron, Kotyo, Japan) were then used to fix the orbital hardware in the internal orbital rim. A forced duction test was performed to confirm that the impinged orbital contents had been released. Finally, the incised periosteum was closed, and the tarsal plates repaired. A drain was placed.

### Statistics analysis

The Wilcoxon signed-rank test was used to analyze the perioperative difference in orbital volume and OVR. A *p*-value <0.05 was considered to indicate significance. All of the analyses were performed using SPSS ver. 20.0 for Windows (SPSS Inc., Armonk, NY, USA).

## RESULTS

The patients (seven males and five females) in the operative group

were aged between 28 and 74 (mean, 49±14). Six patients had an inferomedial blowout fracture. Three had an orbital inferior wall fracture, and the remaining three had a medial orbital wall fracture. The causes of fractures included motor vehicle-related incident in five cases, slip down in three cases, assault in two cases, fall in one case, and an industrial accident in one case (Table 1). Operations were performed at an average of 7.75±2.09 days after having been injured (range, 4 to 13 days). The mean operation time was 117.50±25.18 minutes (ranging from 80 to 155 minutes), and the follow-up lasted for 4–31 weeks (median, 14 weeks). Preoperatively, seven patients had diplopia (2 severe and 5 mild). One patient had enophthalmos. Six patients demonstrated an extraocular movement dysfunction of which four had presented with retrobulbar hemorrhage. Among the 2 out of 4 patients who have retrobulbar hemorrhage with extraocular movement dysfunction were accompanied by traumatic optic neuropathy. Four of the retrobulbar hemorrhage patients had no muscle entrapment in initial radiologic examination, and therefore the operation was carried out after watching progress of observation period. In the sample, the mean orbital volume in the injured side decreased significantly from 27.45±4.81 cm<sup>3</sup> (ranging from 21.32 to 36.60 cm<sup>3</sup>) preoperatively to 24.82±3.93 cm<sup>3</sup> (ranging from 20.04 to 31.42 cm<sup>3</sup>) postop-

**Table 1.** Summary of the subjects included

| Patient | Age (yr) | Sex    | Mecahnism of injury | Time to repair (day) | Orbits involved | Retrobulbar hemorrhage | Other fracture (s) |
|---------|----------|--------|---------------------|----------------------|-----------------|------------------------|--------------------|
| 1       | 74       | Female | MVC                 | 9                    | Inferomedial    | No                     | None               |
| 2       | 55       | Male   | Fall                | 8                    | Inferomedial    | Yes                    | None               |
| 3       | 52       | Female | MVC                 | 7                    | Inferior        | No                     | None               |
| 4       | 42       | Female | Assult              | 8                    | Medial          | Yes                    | None               |
| 5       | 42       | Male   | Work accident       | 7                    | Medial          | No                     | Nasal bone         |
| 6       | 28       | Female | Slip down           | 6                    | Inferior        | No                     | None               |
| 7       | 33       | Male   | MVC                 | 13                   | Inferomedial    | Yes                    | Nasal bone         |
| 8       | 57       | Male   | MVC                 | 8                    | Inferior        | No                     | None               |
| 9       | 70       | Male   | Slip down           | 7                    | Medial          | Yes                    | None               |
| 10      | 50       | Female | MVC                 | 8                    | Inferomedial    | No                     | Nasal bone         |
| 11      | 56       | Male   | Assult              | 4                    | Inferomedial    | No                     | Nasal bone         |
| 12      | 32       | Male   | Slip down           | 8                    | Inferomedial    | No                     | Nasal bone         |

MVC, motor vehicle collision.

**Table 2.** Summary of the orbital volume measurements and orbital volume ratio for unilateral fractures

| Variable  | Fractured side           | Non-fractured side       | Orbital volume ratio (%)   |
|---|--------------------------|--------------------------|----------------------------|
| Preoperative orbital volume (cm <sup>3</sup> )  | 27.45±4.81 (21.32–36.60) | 25.00±3.50 (20.00–31.42) | 109.52±6.62 (99.17–125.09) |
| Postoperative orbital volume (cm <sup>3</sup> ) | 24.82±3.93 (20.04–31.42) | 24.92±3.37 (20.42–29.91) | 99.42±4.67 (93.04–106.80)  |
| <i>p</i> -value                                 | 0.02                     | 0.754                    | 0.02                       |

n=12 subjects, n=12 orbital fractures.

The *p*-values were computed using Wilcoxon signed ranks tests for paired comparisons.

eratively ( $p=0.02$ ). The mean OVR decreased significantly from  $1.0952\pm 0.0662$  (ranging from 0.9917 to 1.2509) preoperatively to  $0.9942\pm 0.0467$  (ranging from 0.9304 to 1.0680) postoperatively ( $p=0.02$ ) (Table 2).

Most patients (11 out of 12) experienced no postoperative complications, such as extraocular movement dysfunction, diplopia, or enophthalmos, during the follow-up. A single patient with preoperative traumatic optic neuropathy experienced immediate postoperative extraocular movement dysfunction and diplopia, which was resolved by 6 months.

## DISCUSSION

As a type of 3D printing, the RP technique started as “additive manufacturing,” which uses computer-aided design and computer-aided manufacture (CAD-CAM) to accumulate the materials layer by layer and manufacture products. This is applied to diverse fields because it can flexibly produce a complex structure from a range of materials, which is in contrast to existing manufacturing techniques such as cutting or molding. The RP technique has attracted increasing interest in the medical field, and has shown to be very useful in the craniofacial field, which is structurally complex [2,4,14].

In 1994, Mankovich et al. [15] first applied a RP model to skull reconstruction. They used a RP model to find a donor of calvarial bones, the curvature of which was appropriate for covering skull defects, and easily succeeded in finding a donor with a similar anatomical structure to that of the patient. For orthognathic surgery, Hibi et al. [16] used a RP model to preoperatively design osteotomy and manufactured a pre-bent titanium plate using a mandible of the RP model segmented during osteosynthesis to improve the surgical accuracy. According to a recent report, a 3D printed titanium-based

implant applicable to a human body was used to reconstruct calvarial and maxillary defects without adverse effects [8,17].

Orbital cavity defect reconstruction is a challenge for operators due to the anatomical complexity, narrow surgical view, and critical contents in the vicinity [13]. Improper operation can lead to complications, such as postoperative diplopia and enophthalmos, and the complications following orbital inferior wall blowout fracture reconstruction reportedly included postoperative diplopia (20%–52%), inferior orbital nerve function defects (55% in single-center studies), and continued enophthalmos (27.5%) [5]. Lim et al. [13] reported that the application of both an endoscope-using transnasal approach and a conventional method in ballooning, and packing paranasal sinus was more effective in reducing the orbital volume than that of the conventional method alone. Gordon et al. [18] reported that the use of a pre-bent titanium implant, considering the three-dimensional orbital anatomy, led to an effective reconstruction. On the other hand, there is no standard method that can provide a consistent outcome, and both a clinically favorable outcome and an ideal type of anatomical restoration may require a good understanding of the individual anatomy of each patient.

Orbital cavity reconstruction is an ideal target of the RP technique owing to its anatomical complexity, and many researchers have applied a RP model to reconstruction [4,6,7,19]. Identifying an anatomical landmark is difficult in cases of large defects due to the thin orbital wall [7,15,19], Kozakiewicz et al. [2] used an uninjured site as a mirrored RP model template to manufacture a pre-bent titanium implant when performing an orbital inferior wall fracture reconstruction. With a mirrored RP model, however, it was impossible to locate defects in the intraoperative field, and disagreement between the pre-bent titanium implant and the defect site may require the implant to be trimmed and redesigned, which increases

the operative time. Therefore, a model that can not only show actual defects of a patient but also be used as a template can be useful.

In this study, CAD based on the mirrored image of the uninjured orbital cavity in a virtual 3D model was used to manufacture both a guide implant and an orbital RP model to cover a defect site. This technique allowed a more accurate surgical plan so that the operator could identify the anatomical defects in the patient and perform the optimal reconstruction.

The RP technique involves (1) CT scanning, (2) CT data processing and virtual 3D model creation, and (3) model production by RP, all of which takes approximately 120 minutes [2]. Virtual 3D modeling can determine the location and size of the orbital cavity defects and the anatomy of individual patients, and preoperative virtual surgical planning may enable greater accuracy in reconstructed contour [10,20]. Three-dimensional measurements are used to determine the variations in the orbital cavity volume, predict potential enophthalmos, even at the early stage of injury, and help determine the operability. The increase in the orbital cavity volume is linearly proportional to enophthalmos. A 1-cm<sup>3</sup> increase in the orbital cavity volume was reported to lead to about 0.77 mm enophthalmos, and a 2.8% increase in the volume could cause 1 mm extraocular movement [21]. In this study, virtual 3D measurements were effective in determining the operability because the mean OVR of 1.0952 ±0.0662 (ranging from 0.9917 to 1.2509) predicted potential enophthalmos, even though one patient had the condition preoperatively.

Intraoperative navigation is the most valuable and effective tool for an operator [2,6]. The tool enables use of the CT and MRI information along with a map in correlation with the anatomy in the operative field as well as good management and protection of the critical contents despite the narrow surgical field [22]. Bell and Markiewicz [6] used a RP model as a template for a bone graft to perform an orbital reconstruction, applied a mirrored navigation system to confirm the optimal position and fixation of the harvested bones, and consequently, repaired large orbital cavity defects effectively.

In this study, a guide implant RP model and a RP model of the orbital cavity were used for preoperative surgical planning, and the guide implant RP model was used as an intraoperative template to identify the anatomical defects correctly and present the optimal

goal. Accurate implant positioning using an intraoperative navigation system decreased the mean orbital cavity volume in the fracture site significantly from 27.45±4.81 cm<sup>3</sup> (ranging from 21.32 to 36.60 cm<sup>3</sup>) preoperatively to 24.82±3.93 cm<sup>3</sup> (ranging from 20.04 to 31.42 cm<sup>3</sup>) postoperatively ( $p=0.02$ ), and decreased the mean OVR from 1.0952±0.0662 (ranging from 0.9917 to 1.2509) preoperatively to 0.9942±0.0467 (ranging from 0.9304 to 1.0680) postoperatively ( $p=0.02$ ) (Fig. 3). This also contributed to the clinical outcome without postoperative enophthalmos or long-term complications.

The cost of RP technique can be variable due to open source software with low cost 3D printer to high cost software and facilities. In this study, the amount of consumable material used for the production was about 200cc in a single model, with the cost as low as \$100 USD. The continuing development of inexpensive and easy to use 3D printers increases the likelihood that this technology will soon have major uses in medicine.

This study has its limitations. It was conducted on only 12 patients with a short-term follow-up. Also, this method is associated with several disadvantages: (1) the length of time required to build model; (2) the cooperation required between a number of people in different locations with additional costs; and (3) the use of this method in panfacial fractures is challenging because it is difficult to find any stable orbital margins for virtual planning of the model and to establish an accurate position for the pre-shaped plates.

In conclusion, the orbital cavity and guide implant RP technique in a unilateral orbital cavity reconstruction gives a good understanding of the anatomical state of the injured orbit, predicts the potential outcome through three-dimensional measurements and helps determine the operability. The technique is effective in restoring the orbital cavity volume through optimal implant positioning along with an intraoperative navigation system. This may help bring about a clinically favorable outcome. The RP technique is expected to ease the difficulty of orbital reconstruction by producing implants through CAD applicable to the human body.

## REFERENCES

1. Park SW, Choi JW, Koh KS, Oh TS. Mirror-imaged rapid prototype skull model and pre-molded synthetic scaffold to achieve optimal or-

- bital cavity reconstruction. *J Oral Maxillofac Surg* 2015;73:1540-53.
2. Kozakiewicz M, Elgalal M, Loba P, Komunski P, Arkuszewski P, Broniarczyk-Loba A, et al. Clinical application of 3D pre-bent titanium implants for orbital floor fractures. *J Craniomaxillofac Surg* 2009;37:229-34.
  3. Gur Y. Additive manufacturing of anatomical models from computed tomography scan data. *Mol Cell Biomech* 2014;11:249-58.
  4. Choi JW, Kim N. Clinical application of three-dimensional printing technology in craniofacial plastic surgery. *Arch Plast Surg* 2015;42:267-77.
  5. Gart MS, Gosain AK. Evidence-based medicine: orbital floor fractures. *Plast Reconstr Surg* 2014;134:1345-55.
  6. Bell RB, Markiewicz MR. Computer-assisted planning, stereolithographic modeling, and intraoperative navigation for complex orbital reconstruction: a descriptive study in a preliminary cohort. *J Oral Maxillofac Surg* 2009;67:2559-70.
  7. Mourits DL, Wolff J, Forouzanfar T, Ridwan-Pramana A, Moll AC, de Graaf P, et al. 3D orbital reconstruction in a patient with microphthalmos and a large orbital cyst: a case report. *Ophthalmic Genet* 2016;37:233-7.
  8. Beliakin SA, Khyshov VB, Khyshov MB, Klimova NA, Saifullina SN, Eizenbraun OV. Reconstruction of posttraumatic skull and facial bones injuries with the use of perforated titanium plates and meshes. *Voen Med Zh* 2012;333:12-7.
  9. Huang W, Zhang X. 3D Printing: print the future of ophthalmology. *Invest Ophthalmol Vis Sci* 2014;55:5380-1.
  10. Winder J, McRitchie I, McKnight W, Cooke S. Virtual surgical planning and CAD/CAM in the treatment of cranial defects. *Stud Health Technol Inform* 2005;111:599-601.
  11. Hur SW, Kim SE, Chung KJ, Lee JH, Kim TG, Kim YH. Combined Orbital Fractures: surgical strategy of sequential repair. *Arch Plast Surg* 2015;42:424-30.
  12. Yano H, Nakano M, Anraku K, Suzuki Y, Ishida H, Murakami R, et al. A consecutive case review of orbital blowout fractures and recommendations for comprehensive management. *Plast Reconstr Surg* 2009;124:602-11.
  13. Lim NK, Kang DH, Oh SA, Gu JH. Orbital wall restoring surgery in pure blowout fractures. *Arch Plast Surg* 2014;41:686-92.
  14. Raphael O, Herve R. Clinical applications of rapid prototyping models in cranio-maxillofacial surgery. Rijeka: INTECH Open Access Publisher; 2011.
  15. Mankovich NJ, Samson D, Pratt W, Lew D, Beumer J 3rd. Surgical planning using three-dimensional imaging and computer modeling. *Otolaryngol Clin North Am* 1994;27:875-89.
  16. Hibi H, Sawaki Y, Ueda M. Three-dimensional model simulation in orthognathic surgery. *Int J Adult Orthodon Orthognath Surg* 1997;12:226-32.
  17. Chen ST, Chang CJ, Su WC, Chang LW, Chu IH, Lin MS. 3-D titanium mesh reconstruction of defective skull after frontal craniectomy in traumatic brain injury. *Injury* 2015;46:80-5.
  18. Gordon CR, Susarla SM, Yaremchuk MJ. Quantitative assessment of medial orbit fracture repair using computer-designed anatomical plates. *Plast Reconstr Surg* 2012;130:698e-705e.
  19. Lim CG, Campbell DI, Clucas DM. Rapid prototyping technology in orbital floor reconstruction: application in three patients. *Craniomaxillofac Trauma Reconstr* 2014;7:143-6.
  20. Susarla SM, Duncan K, Mahoney NR, Merbs SL, Grant MP. Virtual Surgical Planning for Orbital Reconstruction. *Middle East Afr J Ophthalmol* 2015;22:442-6.
  21. Whitehouse RW, Batterbury M, Jackson A, Noble JL. Prediction of enophthalmos by computed tomography after 'blow out' orbital fracture. *Br J Ophthalmol* 1994;78:618-20.
  22. Luebbbers HT, Messmer P, Obwegeser JA, Zwahlen RA, Kikinis R, Graetz KW, et al. Comparison of different registration methods for surgical navigation in cranio-maxillofacial surgery. *J Craniomaxillofac Surg* 2008;36:109-16.